

# [(NH<sub>3</sub>CH<sub>2</sub>CH<sub>2</sub>CH<sub>2</sub>NH<sub>2</sub>CH<sub>2</sub>)<sub>2</sub>]<sub>0.5</sub>[Sb<sub>7</sub>S<sub>11</sub>]: A New Two-Dimensional Antimony Sulfide with Antimony–Antimony Bonding

Anthony V. Powell\* and Sylvain Boissière

Department of Chemistry, Heriot-Watt University, Edinburgh EH14 4AS, U.K.

Ann M. Chippindale†

Chemical Crystallography Laboratory, University of Oxford, 9 Parks Road, Oxford OX1 3PD, U.K.

Received August 13, 1999

A new two-dimensional antimony sulfide has been synthesized under hydrothermal conditions in the presence of *N,N*-bis(3-aminopropyl)ethylenediamine and characterized by single-crystal X-ray diffraction, thermogravimetry and elemental analysis. The product [C<sub>8</sub>N<sub>4</sub>H<sub>26</sub>]<sub>0.5</sub>[Sb<sub>7</sub>S<sub>11</sub>] (*M<sub>r</sub>* = 1294.07) crystallizes in the triclinic space group, *P*1̄, with *a* = 5.9550(3) Å, *b* = 14.567(1) Å, *c* = 15.093(1) Å, α = 68.448(4)°, β = 86.044(6)°, γ = 82.280(6)°, *V* = 1206 Å<sup>3</sup>, and *Z* = 2. The structure consists of infinite chains of formula Sb<sub>7</sub>S<sub>11</sub><sup>2-</sup> linked through antimony–antimony bonds (2.921(2) Å) into two-dimensional slabs of approximate thickness 2.6 Å. These slabs contain pores of dimensions ca. 17.5 × 5.2 Å, which are aligned along the [100] direction. *N,N*-Bis(3-aminopropyl)ethylenediamine cations reside between the slabs to which they are hydrogen bonded.

## Introduction

Microporous solids have attracted considerable attention in recent years.<sup>1</sup> Much of this interest derives from the technologically useful properties that regular networks of channels and cavities, with dimensions in the nanometer range, confer. These structural features give rise to a high degree of selectivity for sorptive and reactive processes, leading to applications as catalysts, ion exchangers, and molecular sieves.<sup>2–5</sup> In the continuing quest for new materials with enhanced properties, template-directed synthesis has been increasingly utilized. The template molecule, typically an organic amine, when added to a gel or slurry of essentially inorganic reactants prior to solvothermal reaction, appears to exert a directing effect on the crystallization process and results in the formation of an open-framework inorganic material in which the organic species is retained within the channels or cavities. This approach has successfully been applied to the synthesis of a wide range of oxide-based microporous materials with novel structures, including a large number of aluminosilicates (zeolites),<sup>6</sup> main-group and transition-metal phosphates,<sup>7,8</sup> and metal–oxide frameworks.<sup>9</sup>

Following a report in 1989 by Bedard and co-workers<sup>10</sup> that a similar strategy can be applied to effect the crystallization of tin and germanium sulfides, there has been considerable interest in the directed solvothermal synthesis of open-framework chalcogenides.<sup>11</sup> The majority of these are sulfides of the main-group elements antimony,<sup>12–19</sup> tin,<sup>20,21</sup> indium,<sup>22,23</sup> and germanium.<sup>24–28</sup>

- (6) Lok, B. M.; Cannan, T. R.; Messina, C. A. *Zeolites* **1983**, 3, 282.
- (7) Cheetham, A. K.; Ferey, G.; Loiseau, T. *Angew Chem., Int Ed. Engl.* **1999**, 38, 3268.
- (8) Haushalter, R. C.; Mundi, L. A. *Chem. Mater.* **1992**, 4, 31.
- (9) Xu, Y. *Curr. Opin. Solid State Mater. Chem.* **1999**, 4, 133.
- (10) Bedard, R. L.; Wilson, S. T.; Vail, L. D.; Bennett, J. M.; Flanigen, E. M. In *Zeolites: Facts, Figures, Future*; Jacobs, P. A., van Santen, R. A., Eds.; Elsevier: Amsterdam, 1989.
- (11) Sheldrick W. S.; Wachhold, M. *Angew. Chem., Intl. Ed. Engl.* **1997**, 36, 206.
- (12) Tan, K.; Ko, Y.; Parise, J. B.; Park, J. B.; Darovsky, A. *Chem. Mater.* **1996**, 8, 2510.
- (13) Parise, J. B.; Ko, Y. *Chem. Mater.* **1992**, 4, 1446.
- (14) Parise, J. B. *Science* **1991**, 251, 293.
- (15) Ko, Y.; Tan, K.; Parise, J. B.; Darovsky, A. *Chem. Mater.* **1996**, 8, 493.
- (16) Tan, K.; Ko, Y.; Parise, J. B. *Acta Crystallogr., Sect C* **1994**, 50, 1439.
- (17) Wang, X.; Liebau, F. *J. Solid State Chem.* **1994**, 111, 385.
- (18) Wang, X.; Jacobson, A. J.; Liebau, F. *J. Solid State Chem.* **1998**, 140, 387.
- (19) Wang, X. *Eur. J. Solid State Inorg. Chem.* **1995**, 32, 303.
- (20) Jiang, T.; Lough, A.; Ozin, G. A.; Bedard, R. L.; Broach, R. J. *Mater. Chem.* **1998**, 8, 721.
- (21) Jiang, T.; Ozin, G. A. *J. Mater. Chem.* **1998**, 8, 1099.
- (22) Cahill, C. L.; Younghee, K.; Parise, J. B. *Chem. Mater.* **1998**, 10, 19.
- (23) Cahill, C. L.; Gugliotta, B.; Parise, J. B. *Chem. Commun.* **1998**, 1715.
- (24) Tan, K.; Darovsky, A.; Parise, J. B. *J. Am. Chem. Soc.* **1995**, 117, 7039.
- (25) Krebs, B. *Angew. Chem., Intl. Ed. Engl.* **1983**, 22, 113.
- (26) MacLachlan, M.; Coombs, N.; Ozin, G. A. *Nature* **1999**, 397, 681.
- (27) Cahill, C. L.; Parise, J. B. *Chem. Mater.* **1997**, 9, 807.

\* To whom correspondence should be addressed. Fax: +44 (0)131 451 3180. E-mail: a.v.powell@hw.ac.uk.

† Present address: Department of Chemistry, The University of Reading, Whiteknights, Reading RG6 6AD, Berkshire, U.K.

(1) Davis, M. E. *Acc. Chem. Res.* **1993**, 26, 111.  
 (2) Thomas, J. M. *Angew Chem., Intl. Ed. Engl.* **1994**, 33, 913.  
 (3) Davis, M. E. *Microporous Mesoporous Mater.* **1998**, 21, 173.  
 (4) Barrer, R. M. *Zeolites and Clay Minerals as Sorbents and Molecular Sieves*; Academic Press: London, 1978.  
 (5) Ozin, G. A.; Kuperman, A.; Stein, A. *Angew Chem., Int Ed. Engl.* **1989**, 28, 359.

The different bonding preferences of sulfur compared with oxygen give rise to a variety of complex building units, including the  $\text{Sb}_3\text{S}_6^{3-}$  semicube,<sup>12,13,15,16,29</sup> the  $\text{Ge}_4\text{S}_{10}^{4-}$  adamantane unit,<sup>26,27</sup> and the  $\text{In}_{10}\text{S}_{20}^{10-}$  supertetrahedron,<sup>22</sup> which in turn link to produce novel metal-sulfur networks. In particular, the sulfides exhibit a greater tendency for reduced framework dimensionality than their oxide counterparts. This is exemplified by the antimony sulfides which exhibit a variety of chainlike structural motifs derived from vertex-linked  $\text{Sb}_3\text{S}_3^{3-}$  pyramidal species. The  $\text{Sb}_4\text{S}_7^{2-}$  chain, in particular, occurs in a number of structures, either isolated<sup>13,30,31</sup> or linked by a variety of bridging units to form double chains such as  $\text{Sb}_8\text{S}_{13}^{2-}$ ,<sup>16</sup>  $\text{Sb}_{10}\text{S}_{16}^{2-}$ ,<sup>19</sup> and  $\text{Sb}_8\text{S}_{14}^{2-}$ .<sup>12</sup> The last structure also contains a persulfide linkage. Interlocking of these, or similar chains, may produce two- or even three-dimensional structures. While all of these materials possess relatively open antimony-sulfide frameworks, apparently minor changes in framework density have a marked effect on the colors of the product materials which range from dark red at high density to yellow in the most open structures. These colors indicate a considerable increase in the band gap over that of  $\text{Sb}_2\text{S}_3$  (1.7 eV), suggesting that the materials may possess interesting optical properties.

Here we report the synthesis and structure determination of a new antimony sulfide,  $[\text{C}_8\text{N}_4\text{H}_{26}]_{0.5}[\text{Sb}_7\text{S}_{11}]$  synthesized under hydrothermal conditions using a long-chain amine as template. The structure consists of  $\text{Sb}_7\text{S}_{11}^{2-}$  chains linked by Sb-Sb bonds to form a two-dimensional sheet in which there are rectangular pores. Alignment of pores in successive sheets confers one-dimensional tunnelike characteristics on the structure.

### Experimental Section

**Synthesis and Characterization.** The structure-directing agent, *N,N*-Bis(3-aminopropyl)ethylenediamine, was pretreated by bubbling  $\text{H}_2\text{S}$  through it for 3 h prior to use. The amine (0.6 mL) and water (1.6 mL) were then added to  $\text{Sb}_2\text{S}_3$  (0.83 g), with stirring, to produce a slurry of approximate molar composition  $\text{Sb}_2\text{S}_3$ :amine:water of 1:1:30. The slurry was sealed into a Teflon-lined stainless steel autoclave, heated at 473 K for a period of 3 days and then cooled slowly at 1 K  $\text{min}^{-1}$ . The solid product, which was collected by filtration, washed with deionized water and ethanol and then dried in air, consisted of a mixture of dark-red/black needles and black polycrystalline material. The latter was subsequently identified as unreacted antimony sulfide. Extending the reaction time to 7 days led to complete reaction and a solid product which consisted exclusively of dark-red/black needles. Powder X-ray diffraction analysis of a ground sample of this product was performed on a Philips PA2000 powder diffractometer using Ni-filtered  $\text{Cu K}\alpha$  radiation ( $\lambda = 1.5418 \text{ \AA}$ ). All peaks in the powder diffraction pattern (Figure 1) could be indexed on the basis of the triclinic unit cell determined from the single-crystal X-ray diffraction study with refined unit-cell parameters  $a = 5.960(5) \text{ \AA}$ ,  $b = 14.544(2) \text{ \AA}$ ,  $c = 15.077(6) \text{ \AA}$ ,  $\alpha = 68.4(1)^\circ$ ,  $\beta = 86.0(2)^\circ$ ,  $\gamma = 82.3(1)^\circ$ .

Combustion analysis of the bulk material gave the following results: C, 3.29; H, 0.85; N, 1.76%, which compare favorably

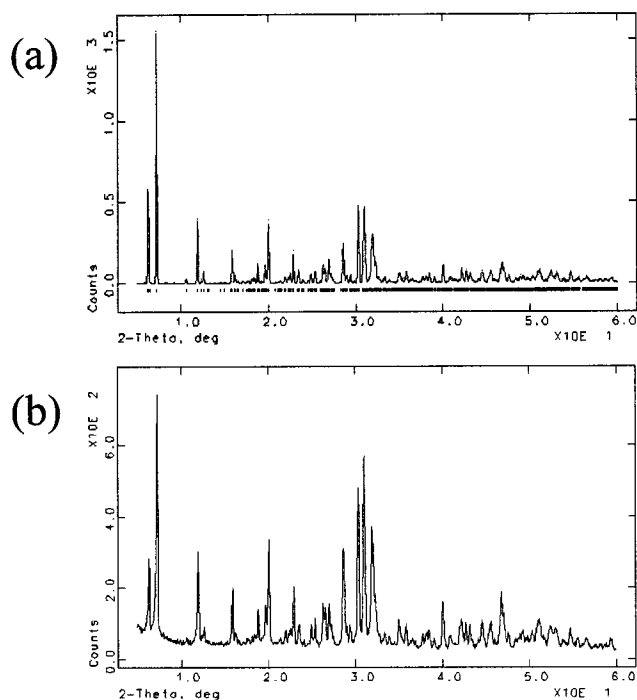


**Figure 1.** Powder X-ray diffraction data for  $[\text{C}_8\text{N}_4\text{H}_{26}]_{0.5}[\text{Sb}_7\text{S}_{11}]$ : (a) calculated pattern generated from the structure determined by single-crystal X-ray diffraction (reflection positions are marked); (b) experimental data.

with values calculated from the crystallographically determined formula  $[\text{C}_8\text{N}_4\text{H}_{26}]_{0.5}[\text{Sb}_7\text{S}_{11}]$  (C, 3.71; H, 1.01; N, 2.16%). Thermogravimetric analysis was performed using a DuPont Instruments 951 thermal analyzer. Approximately 24 mg of single crystals was heated under a flow of nitrogen over the temperature range 293–563 K at a heating rate of 5 K  $\text{min}^{-1}$ . A gradual weight loss of 7.84% observed at 533–558 K is consistent with the simultaneous removal of the organic component and half a mole of sulfur per formula unit (calculated 7.97%) to yield  $\text{Sb}_2\text{S}_3$ , the identity of which was confirmed by powder X-ray diffraction. Analytical electron microscopy was performed on ground single crystals, coated with carbon to eliminate charging effects, using a Hitachi S-2700 scanning electron microscope fitted with a PGT IMIX-XE detection system. Using  $\text{Sb}_2\text{S}_3$  as an intensity standard, an antimony:sulfur ratio of 0.60(2) was obtained. This is in good agreement with the value of 0.64 calculated for the crystallographically determined composition.

**Single-Crystal Structure Determination.** A dark-red/black needle of  $[\text{C}_8\text{N}_4\text{H}_{26}]_{0.5}[\text{Sb}_7\text{S}_{11}]$  with dimensions  $0.02 \times 0.09 \times 0.40 \text{ mm}$  was mounted on a thin glass fiber using cyanoacrylate adhesive. X-ray diffraction data were collected at 293 K using an Enraf-Nonius DIP2020 image-plate diffractometer (graphite-monochromated  $\text{Mo K}\alpha$  radiation ( $\lambda = 0.7107 \text{ \AA}$ )). Images were processed using the DENZO and SCALEPACK suite of programs.<sup>32</sup> Data were corrected for Lorentz and polarization effects, and a partial absorption correction was applied by multiframe scaling of the image-plate data using equivalent reflections. The crystal was determined to be triclinic with lattice parameters  $a = 5.9550(3) \text{ \AA}$ ,  $b = 14.567(1) \text{ \AA}$ ,  $c = 15.093(1) \text{ \AA}$ ;  $\alpha = 68.448(4)^\circ$ ,  $\beta = 86.044(6)^\circ$ ,  $\gamma = 82.280(6)^\circ$  and unit-cell volume  $1206.42 \text{ \AA}^3$ . Crystallographic data are summarized in Table 1.

The structure was solved in space group  $P\bar{1}$  by direct methods using the program SIR-92,<sup>33</sup> which located all of the

(28) Bowes, C. L.; Huynh, W. U.; Kirkby, S. J.; Malek, A.; Ozin, G. A.; Petrov, S.; Twardowski, M.; Young, D.; Bedard, R. L.; Broach, R. *Chem. Mater.* **1996**, *8*, 2147.

(29) Parise, J. B. *J. Chem. Soc., Chem. Commun.* **1990**, 1553.

(30) Bensch, W.; Schur, M. *Z. Naturforschung.* **1997**, *52b*, 405.

(31) Stephan, H. O.; Kanatzidis, M. G. *Inorg. Chem.* **1997**, *36*, 6050.

(32) Otwinowski, Z.; Minor, W. In *Methods in Enzymology*; Carter, C. W., Sweet, R. M., Eds.; Academic Press: New York, 1997, p 276.

(33) Altomare, A.; Burla, M. C.; Camalli, M.; Cascarano, G.; Giacovazzo, G.; Guargliardi, A.; Polidori, G. *J. Appl. Crystallogr.* **1994**, *27*, 435.

**Table 1. Crystallographic Data for [C<sub>8</sub>N<sub>4</sub>H<sub>26</sub>]<sub>0.5</sub>[Sb<sub>7</sub>S<sub>11</sub>]**

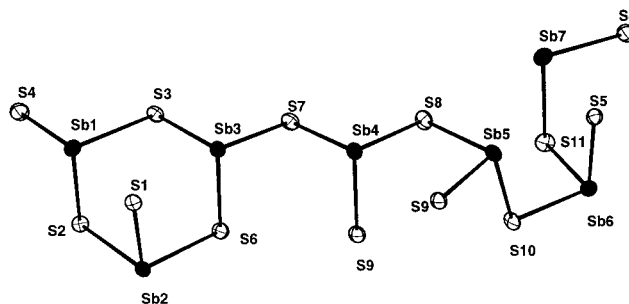
formula	C <sub>4</sub> N <sub>2</sub> H <sub>13</sub> Sb <sub>7</sub> S <sub>11</sub>
<i>M<sub>r</sub></i>	1294.07
cryst size (mm)	0.02 × 0.09 × 0.40
cryst habit	dark-red/black needle
cryst syst	triclinic
space group	<i>P</i> $\bar{1}$
<i>a</i> (Å)	5.9550(3)
<i>b</i> (Å)	14.567(1)
<i>c</i> (Å)	15.093(1)
$\alpha$ (deg)	68.448(4)
$\beta$ (deg)	86.044(6)
$\gamma$ (deg)	82.280(6)
unit-cell vol (Å <sup>3</sup> )	1206.42
<i>Z</i>	2
$\rho_{\text{calc}}$ (g cm <sup>-3</sup> )	3.56
$\mu$ (cm <sup>-1</sup> )	86.99
radiation	Mo K $\alpha$ ( $\lambda$ = 0.7107 Å)
temp (K)	293
$\theta_{\text{max}}$ (deg)	26.57
unique data	4628
obsd data ( <i>I</i> > 6 $\sigma$ ( <i>I</i> ))	2956
<i>R<sub>merg</sub></i>	0.052
no. of params refined	217
residual electron density (e Å <sup>-3</sup> )	-2.55, +2.23
<i>R</i>	0.046 <sup>a</sup>
<i>R<sub>w</sub></i>	0.044 <sup>a</sup>

<sup>a</sup> Refinement against *F*.**Table 2. Fractional Atomic Coordinates and Equivalent Isotropic Thermal Parameters for Non-hydrogen Atoms in [C<sub>8</sub>N<sub>4</sub>H<sub>26</sub>]<sub>0.5</sub>[Sb<sub>7</sub>S<sub>11</sub>]**

atom	<i>x</i>	<i>y</i>	<i>z</i>	<i>U</i> (iso) (Å <sup>2</sup> )
Sb(1)	-0.4215(2)	-0.36939(6)	0.60224(7)	0.0221
Sb(2)	0.1400(2)	-0.53737(7)	0.63184(6)	0.0191
Sb(3)	-0.3647(2)	-0.63903(7)	0.79574(6)	0.0198
Sb(4)	-0.3023(2)	-0.89071(7)	0.98465(6)	0.0199
Sb(5)	-0.2358(2)	-0.14640(7)	0.18005(6)	0.0207
Sb(6)	0.0734(2)	-0.23605(6)	0.41920(6)	0.0188
Sb(7)	-0.4905(2)	-0.08022(7)	0.46316(7)	0.0245
S(1)	-0.2247(6)	-0.5555(2)	0.5827(2)	0.0176
S(2)	-0.0283(6)	-0.3619(2)	0.6302(2)	0.0196
S(3)	-0.4890(6)	-0.4679(2)	0.7875(2)	0.0222
S(4)	-0.5304(7)	-0.2010(3)	0.6252(3)	0.0260
S(5)	-0.2992(6)	-0.2735(2)	0.4020(2)	0.0199
S(6)	0.0439(6)	-0.6316(2)	0.8055(2)	0.0204
S(7)	-0.4002(7)	-0.7142(3)	0.9741(2)	0.0247
S(8)	-0.3580(7)	-0.9641(3)	1.1563(2)	0.0235
S(9)	0.1094(6)	-0.8872(3)	0.9887(2)	0.0217
S(10)	0.1359(6)	-0.1489(3)	0.2386(2)	0.0207
S(11)	-0.0805(6)	-0.0836(2)	0.4556(3)	0.0236
N(1)	-0.938(4)	0.134(1)	0.310(1)	0.0655
N(2)	-0.987(3)	0.434(1)	0.1325(9)	0.0377
C(1)	-0.913(4)	0.152(2)	0.213(2)	0.0659
C(2)	-0.860(4)	0.261(2)	0.154(2)	0.0543
C(3)	-1.050(4)	0.330(1)	0.154(1)	0.0538
C(4)	-0.905(3)	0.481(1)	0.035(1)	0.0231

framework Sb and S atoms. The nitrogen and carbon atoms of the template were located in a difference Fourier map. The hydrogen atoms of the template were placed geometrically after each cycle of refinement. All Fourier calculations and subsequent full-matrix least-squares refinements were carried out using the CRYSTALS suite of programs.<sup>34</sup> In the final cycle of refinement, all non-hydrogen atoms were refined anisotropically. A three-term Chebyshev polynomial weighting scheme was applied, and the refinement converged to give final residuals of *R* = 4.61% and *R<sub>w</sub>* = 4.36%. The atomic coordinates and isotropic thermal parameters of non-hydrogen atoms and selected bond lengths and angles are given in Tables 2 and 3, respectively, and the local coordination of the framework atoms is shown in Figure 2.

(34) Watkin, D. J.; Prout, C. K.; Carruthers, R. J.; Betteridge, P.; CRYSTALS, issue 10; Chemical Crystallography Laboratory: Oxford, U.K., 1996.

**Figure 2.** Local coordination of the framework atoms showing the atom labeling scheme and ellipsoids at 50% probability.

## Results and Discussion

Formal valence considerations imply that all Sb atoms are trivalent with the exception of Sb(7), which appears to be divalent, suggesting that either H<sub>2</sub>S or the amine is acting as a reducing agent. Bond-valence sums support these assignments,<sup>35</sup> which result in two negative charges on the inorganic framework.

With the exception of Sb(7), each of the crystallographically unique antimony atoms is coordinated to three sulfur atoms at distances in the range 2.407(4)–2.663(3) Å. These SbS<sub>3</sub> primary structural units have an approximately trigonal pyramidal geometry with S–Sb–S angles in the range 88.4(1)–98.7(1)°. All the antimony atoms have additional sulfur neighbors at longer distances of 2.913(3)–3.797(4) Å, less than the sum of the Sb and S van der Waals' radii (3.80 Å).<sup>36</sup> The presence of short and long Sb–S bonds is frequently encountered in antimony sulfides and has been observed in a number of templated structures, including [N(C<sub>3</sub>H<sub>7</sub>)<sub>4</sub>][Sb<sub>3</sub>S<sub>5</sub>],<sup>13</sup> [CH<sub>3</sub>NH<sub>3</sub>]<sub>2</sub>[Sb<sub>8</sub>S<sub>13</sub>],<sup>16</sup> and [H<sub>3</sub>N(CH<sub>2</sub>)<sub>3</sub>-NH<sub>3</sub>][Sb<sub>10</sub>S<sub>16</sub>].<sup>19</sup> The longer interactions serve to link together higher structural units. The initial discussion of the structure will focus on the primary SbS<sub>3</sub> units. Three of these trigonal pyramids (involving Sb(1) to Sb(3)) are vertex linked to form a puckered six-membered Sb<sub>3</sub>S<sub>6</sub><sup>3-</sup> ring (Figure 3) in chair conformation. This structural moiety, termed a "semicube", has been identified as a secondary building unit in Sb<sub>2</sub>S<sub>3</sub><sup>37</sup> and a number of other templated antimony sulfides, including Sb<sub>4</sub>S<sub>7</sub><sup>2-</sup> chains.<sup>13,30,31</sup> In the present case, semicubes are connected by Sb<sub>8</sub>S<sub>10</sub><sup>2+</sup> linkages to form "double" chains of overall formula Sb<sub>7</sub>S<sub>11</sub><sup>2-</sup> directed along the vector [01–1]. Within the Sb<sub>8</sub>S<sub>10</sub><sup>2+</sup> unit, each Sb(7) atom is coordinatively unsaturated, there being only two short bonds to sulfur (S(4) at 2.450(4) Å and S(11) at 2.432(4) Å). However, the distance between Sb(7) atoms located in adjacent chains is only 2.921(2) Å, suggesting that there is significant interchain metallic bonding. For comparison, Sb–Sb distances of 2.91 and 3.36 Å have been observed in elemental  $\alpha$ -Sb<sup>38</sup> and distances in the range 2.73–2.91 Å in a variety of antimony cluster anions, e.g., Sb<sub>4</sub>S<sub>6</sub><sup>2-</sup>,<sup>39</sup> Sb<sub>7</sub><sup>3-</sup>,<sup>40</sup> and Sb<sub>4</sub>Te<sub>4</sub><sup>4-</sup>.<sup>41</sup>

(35) Brese, N. E.; O'Keeffe, M. *Acta Crystallogr.* **1991**, *B47*, 192.

(36) Bondi, A. J. *Phys. Chem.* **1964**, *68*, 441.

(37) Bayliss, P.; Nowacki, W. Z. *Kristallogr.* **1972**, *135*, 308.

(38) Barrett, C. S.; Cucka, P.; Haefner, K. *Acta Crystallogr.* **1963**, *16*, 451.

(39) Martin, T. M.; Schimek, G. L.; Pennington, W. L.; Kolis, J. W. *J. Chem. Soc., Dalton Trans.* **1995**, 501.

(40) Critchlow, S. C.; Corbett, J. D. *Inorg. Chem.* **1984**, *23*, 770.

(41) Warren, C. J.; Ho, D. M.; Haushalter, R. C.; Bocarsly, A. B. *Angew. Chem., Intl. Ed. Engl.* **1993**, *32*, 1646.

Table 3. Selected Bond Lengths (Å), Bond Valences (vu), and Angles (deg) for  $[\text{C}_8\text{N}_4\text{H}_{26}]_{0.5}[\text{Sb}_7\text{S}_{11}]^{\dagger}$ 

		$\nu^h$			$\nu^h$
Sb(1)–S(2)	2.431(4)	1.05	Sb(5)–S(10)	2.430(4)	1.06
Sb(1)–S(4)	2.593(4)	0.68	Sb(5)–S(9)	2.493(3)	0.89
Sb(1)–S(3)	2.663(3)	0.56	Sb(5)–S(8) <sup>d</sup>	2.555(4)	0.75
Sb(1)–S(5)	2.913(3)	0.29	Sb(5)–S(5)	3.201(3)	0.13
Sb(1)–S(1)	2.914(3)	0.29	Sb(5)–S(6) <sup>b</sup>	3.215(3)	0.13
Sb(1)–S(2') <sup>a</sup>	3.601(4)	0.05	Sb(5)–S(10) <sup>a</sup>	3.787(4)	0.03
sum		2.92	sum		2.99
Sb(2)–S(1)	2.420(4)	1.08	Sb(6)–S(5)	2.407(4)	1.12
Sb(2)–S(6)	2.538(3)	0.79	Sb(6)–S(11)	2.520(3)	0.83
Sb(2)–S(2)	2.609(3)	0.65	Sb(6)–S(10)	2.573(3)	0.72
Sb(2)–S(5) <sup>b</sup>	3.002(3)	0.23	Sb(6)–S(1) <sup>b</sup>	3.060(3)	0.19
Sb(2)–S(1') <sup>b</sup>	3.051(3)	0.20	Sb(6)–S(2)	3.100(3)	0.17
Sb(2)–S(1'') <sup>c</sup>	3.797(4)	0.03			
sum		2.98	sum		3.03
Sb(3)–S(3)	2.463(4)	0.97	Sb(7)–S(7) <sup>f</sup>	2.921(2)	
Sb(3)–S(6)	2.467(4)	0.96	Sb(7)–S(11)	2.432(4)	1.05
Sb(3)–S(7)	2.512(3)	0.85	Sb(7)–S(4)	2.450(4)	1.00
Sb(3)–S(1)	3.089(3)	0.18	Sb(7)–S(5)	3.314(3)	0.10
Sb(3)–S(10) <sup>b</sup>	3.409(4)	0.08	Sb(7)–S(11') <sup>a</sup>	3.530(4)	0.05
Sb(3)–S(6) <sup>a</sup>	3.504(4)	0.06	Sb(7)–S(11'') <sup>g</sup>	3.716(4)	0.03
sum		3.10	sum		2.23
Sb(4)–S(8)	2.431(3)	1.05			
Sb(4)–S(9)	2.464(4)	0.96			
Sb(4)–S(7)	2.507(4)	0.86			
Sb(4)–S(9') <sup>d</sup>	3.171(4)	0.14			
Sb(4)–S(10) <sup>b</sup>	3.307(3)	0.10			
Sb(4)–S(9'') <sup>a</sup>	3.494(4)	0.06			
sum		3.17			
S(2)–Sb(1)–S(3)	90.4(1)		S(8) <sup>e</sup> –Sb(5)–S(9)	95.0(1)	
S(2)–Sb(1)–S(4)	89.2(1)		S(8) <sup>e</sup> –Sb(5)–S(10)	94.3(1)	
S(3)–Sb(1)–S(4)	90.8(1)		S(9)–Sb(5)–S(10)	95.8(1)	
S(1)–Sb(2)–S(2)	88.4(1)		S(5)–Sb(6)–S(10)	93.5(1)	
S(1)–Sb(2)–S(6)	91.5(1)		S(5)–Sb(6)–S(11)	92.9(1)	
S(2)–Sb(2)–S(6)	96.2(1)		S(10)–Sb(6)–S(11)	97.5(1)	
S(3)–Sb(3)–S(6)	96.1(1)		Sb(7)–Sb(7)–S(4)	90.56(9)	
S(3)–Sb(3)–S(7)	94.5(1)		Sb(7)–Sb(7)–S(11)	87.42(9)	
S(6)–Sb(3)–S(7)	90.9(1)		S(4)–Sb(7)–S(11)	98.7(1)	
S(7)–Sb(4)–S(8)	95.5(1)				
S(7)–Sb(4)–S(9)	94.1(1)				
S(8)–Sb(4)–S(9)	95.8(1)				

<sup>a–g</sup> Symmetry transformations used to generate equivalent atoms: (a)  $x - 1, y, z$ ; (b)  $-x, -1 - y, 1 - z$ ; (c)  $1 + x, y, z$ ; (d)  $-x, -2 - y, 2 - z$ ; (e)  $x, 1 + y, z - 1$ ; (f)  $-1 - x, -y, 1 - z$ ; (g)  $-2 - x, 1 - y, 1 - z$ . <sup>h</sup> Bond valences and their sums calculated using parameters from ref 35.

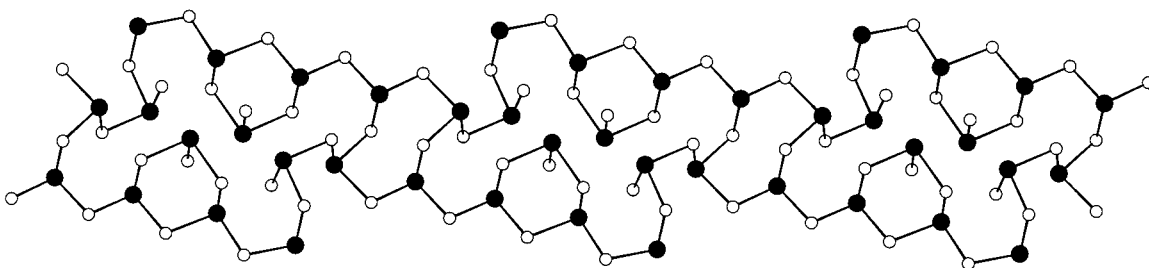


**Figure 3.**  $[\text{Sb}_7\text{S}_{11}]^{2-}$  double chain running parallel to  $[01\bar{1}]$  generated from  $\text{Sb}_3\text{S}_6^{3-}$  semicubes and  $\text{Sb}_8\text{S}_{10}^{2+}$  units: antimony, solid circles; sulfur, open circles.

The Sb(7)–Sb(7) interactions link individual  $\text{Sb}_7\text{S}_{11}^{2-}$  chains into a two-dimensional slab parallel to the (111) plane (Figure 4) with an effective thickness of ca. 2.6 Å. Within each slab are elongated pores bound by 26 alternating Sb and S atoms with dimensions of ca.  $17.5 \times 5.2$  Å, as measured for Sb(7)⋯Sb(7') and S(3)⋯S(7), respectively, giving an effective pore size of ca.  $14 \times 2$  Å on subtraction of appropriate van der Waals' radii. Template molecules, which are tetraprotonated in order to balance the charge of the framework,

reside between the slabs directly below the pores (Figure 5). Both primary and secondary nitrogen atoms of the amine have four nearest sulfur neighbors in the framework at distances in the range of 3.30(1)–3.40(2) Å, implying the possible presence of hydrogen bonding between the template and the framework.

In addition to the "primary" short Sb–S interactions (<2.7 Å), longer "secondary" Sb–S bonds provide additional bonding interactions. In particular, there are weak Sb–S bonds in the range 2.913(3)–3.409(4) Å

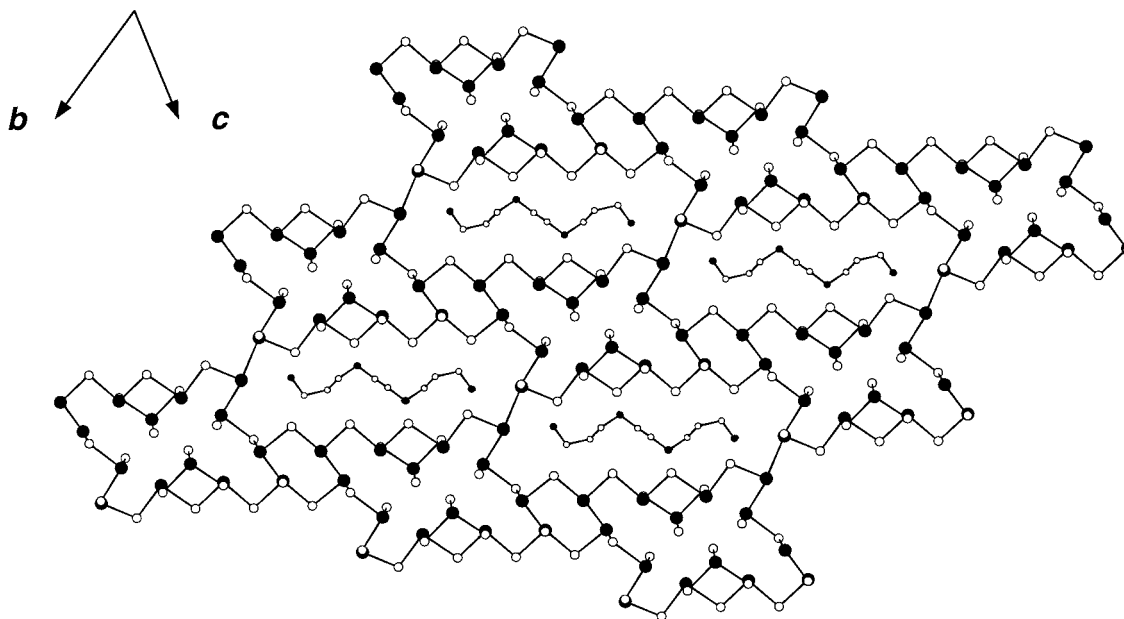


**Figure 4.** View along [100] showing the linkage of  $[\text{Sb}_7\text{S}_{11}]^{2-}$  double chains by Sb(7)–Sb(7) bonds to form two-atom-thick sheets parallel to the (111) plane: antimony, larger solid circles; sulfur, larger open circles; nitrogen, small solid circles; carbon, small open circles. Hydrogen atoms of the template are omitted for clarity.

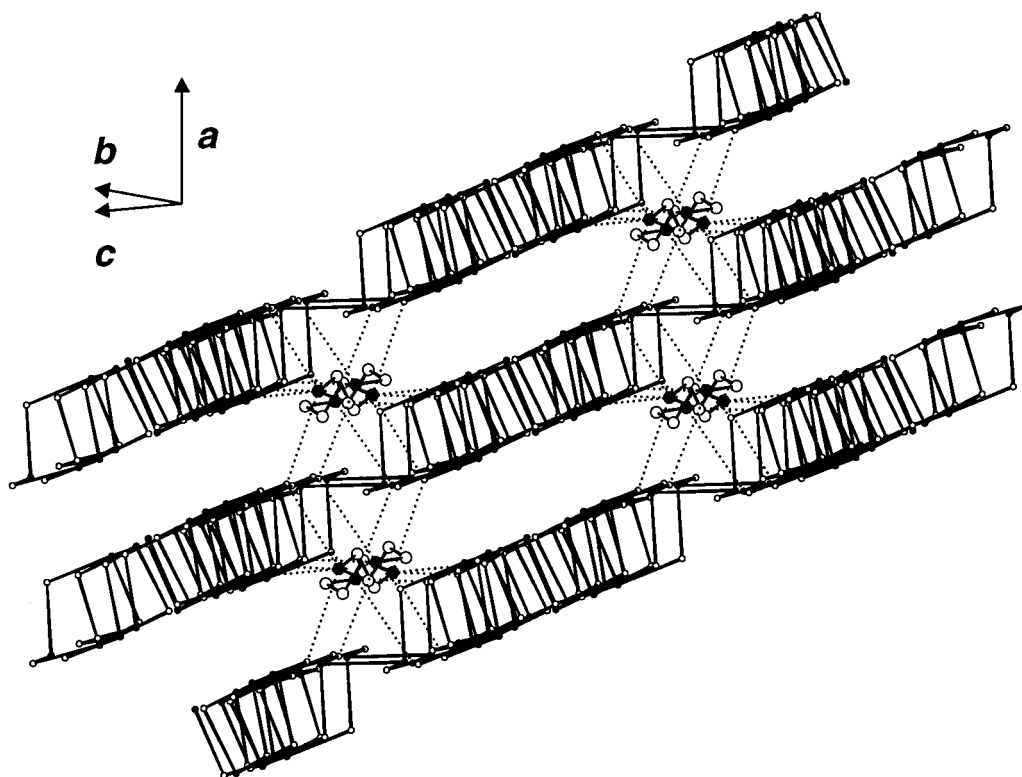


**Figure 5.** Location of the tetraprotonated template between antimony sulfide layers: sulfur, smaller open circles; antimony, smaller solid circles; nitrogen, larger solid circles; carbon, larger open circles. Dotted lines show short sulfide–nitrogen distances (3.30(1)–3.40(2) Å) and indicate a possible network of hydrogen bonds. Hydrogen atoms of the template are omitted for clarity.

within the chains and 3.494(4)–3.797(4) Å between the slabs. The latter interactions, together with those of the amine-framework hydrogen bonds, lead to alignment of the pores in successive slabs. This produces one-dimensional channels in the [100] direction which are occluded by the protonated template molecules.

Antimony sulfides synthesized by solvothermal methods commonly contain chains of fused antimony–sulfur rings, similar to those present in the material reported

here. However, the overall dimensionality of the structure depends on the manner in which such chains interact. Protonated template molecules may act as an organic spacer, keeping neighboring chains sufficiently well-separated that the structure may be regarded as being one-dimensional, as occurs in  $[\text{N}(\text{C}_3\text{H}_7)_4][\text{Sb}_3\text{S}_5]$ , where the shortest interchain Sb–S distances are ca. 7.1 Å.<sup>13</sup> More commonly, there is some degree of interchain interaction via the additional longer Sb–S

bonds. These weaker secondary interactions link chains to form two-dimensional sheets, as found for example in  $[\text{C}_2\text{H}_8\text{N}]_2[\text{Sb}_8\text{S}_{14}]^{12}$  and  $[\text{C}_2\text{H}_{10}\text{N}_2][\text{Sb}_8\text{S}_{13}]^{16}$ . Although more complex two- and three-dimensional structures resulting from linkage of antimony sulfide units by strong primary Sb–S bonds have been observed,<sup>14,15,17</sup> the present compound, with a stoichiometry which has not previously been reported, appears to be the first example in which a two-dimensional structure results from the formation of Sb–Sb bonds. The ability of antimony to form metal–metal bonds, coupled with its tendency to engage in secondary interactions in addition to those in the primary structural units, suggests that antimony chalcogenides could exhibit an even greater

structural diversity than that of the oxide-based materials.

**Acknowledgment.** The assistance of Mr. A. Cowley, University of Oxford, with the data collection and of Dr. P. Vaqueiro, Heriot-Watt University, with the analytical electron microscopy is gratefully acknowledged.

**Supporting Information Available:** Tables listing all bond distances and angles, anisotropic thermal parameters for non-hydrogen atoms, and structure factors and a figure showing the  $[\text{C}_8\text{H}_4\text{H}_{26}]_{0.5}[\text{Sb}_7\text{S}_{11}]$  structure. This material is available free of charge via the Internet at <http://pubs.acs.org>.

CM990526M